3D Shape Measurement Using OFDR

Takanori Saitoh

[Summary] Shape measurement is transitioning from contact methods using Vernier calipers, etc., to non-contact optical methods. These optical methods are based either on time-of-flight or interferometry technologies, but each has problems with precision and measurement range, and meeting requirements for high precision measurement in the range of several centimeters to meters is difficult. As an alternative to these methods, we have developed an OFDR-type distance measurement system supporting seamless measurement over this range with µm-order precision. We used a high-coherence wavelength swept light source developed by Anritsu Devices as the key light source used by OFDR for continuous phase-sweeping of wavelength. Using the advantages of this wavelength swept light source, we were able to measure absolute distance ranges from 0 to 3 m from the collimator lens origin with a precision of 0.2 µm. In addition, we built a 3D shape measurement system for measuring the shape of target objects by scanning up/down and left/right relative to the collimator lens direction. This article presents the shape measurement results and discusses some applications.

1 Introduction

Measurement of an object's shape is a requirement in many different fields, such as diecasting, external inspection of machined products, solder inspection of printed-circuit boards, etc. Another recent application is in Laser Imaging Detection and Ranging (LiDAR) used by self-driving vehicles to measure the shape of objects when mapping roads.

Previous procedures frequently used contact measurement methods with Vernier calipers and micrometers but are now transitioning to non-contact methods using ultrasound and optical technologies.

Time of Flight (ToF) methods measure distance from the time taken for ultrasound or light aimed at the object to return to the source, and LiDAR used by self-driving vehicles is a key technology now in active development worldwide. However, although methods with a measurement resolution of about 10 cm at ranges over 100 m are useful for mapping roads and measuring large-scale structures, they cannot be used in fields requiring better than mm-scale precision for external inspection of products.

Optical interference methods can measure distance from the interference fringe with nm-order precision and are useful for finding small irregularities such as concavities, convexities, and scratches in flat surfaces, but measurement targets are limited to small objects because the depth of field is only a few mm.

More recently, Optical Frequency Domain Reflectometry (OFDR) has been the focus of attention as a high-precision measurement method covering the several centimeter to several meter distance range that has been difficult to measure using previous methods described above.

OFDR has been used previously to measure transmission losses and locations of points generating reflections in optical fibers. As a method for measuring the distribution of propagation loss, there is OTDR (Optical Time Domain Reflectometry) which has the same principle as TOF. However, since the distance resolution for this application is about 1 m, the method cannot be applied for observing reflections in devices using short optical fibers, and in optical devices themselves. On the other hand, since OFDR can achieve a distance resolution of just a few µm, it can be used to measure the distribution of transmission losses within optical devices.

The OFDR method uses a light source for wavelength sweeping but requires a coherence length equal to the measurement range. However, since the distance resolution is inversely proportional to the wavelength sweep width, a wider wavelength sweep width is required. In addition, assuring reliable measurement results requires phase-continuous wavelength sweeping. In other words, a light source is required covering a wide wavelength band without mode hopping and supporting wavelength sweeping while maintaining high coherence.

Although there are extant wavelength light sources meeting these conditions, the sweep speed is about 100 nm/s[1] and the sweep frequency is around 1 Hz. OFDR using a light source with this type of slow sweep frequency would be unable to observe dynamic changes due to vibration.

Anritsu Devices has developed and manufactured[2), 3)] a high-speed wavelength sweeping light source using Micro Electro Mechanical Systems (MEMS) technology (Figure 1). This light source uses a MEMS movable mirror for wavelength sweeping and features high speed and long life. Additionally, it can sweep almost the entire wavelength bandwidth without mode hopping. Table 1 lists the key specifications of this light source.

Figure 1 MEMS Wavelength Swept Light Source

Table 1 Wavelength Swept Light Source Specifications

Center Wavelength λc	1060 nm, 1550 nm
Swept Wavelength Width W	15 to 50 nm (λc: 1060 nm) 30 to 110 nm (λc: 1550 nm)
Sweep Frequency f_R	150 Hz, 1250 Hz
Optical Output Power	>10 dBm
Coherence Length	>100 m (f_R: 150 Hz, W: 40 nm) >10 m (f_R: 1250 Hz, W: 40 nm)

With OFDR, since the light from the light source strikes the measurement target and returns, the measurement range is one-half of the coherence length. There are two types of MEMS wavelength-sweeping light source: a low-speed 150-Hz sweep frequency model, and a high-speed 1250-Hz sweep-frequency model. Since the low-speed model has a minimum coherence length of 100 m, the measurement range is at least 50 m; similarly, the high-speed model has a minimum range of at least 5 m.

Although OFDR was used previously for measuring the distribution of reflections in optical fibers, if the light propagates in free space, it can also measure the distribution of reflection points in free space. For example, the distance to a target can be measured by observing light reflected from the surface of the target; if light reflected from the back face of a target after passing through the surface is measured, the difference in the distance to the surface and back face can be measured as the target thickness. Furthermore, scanning in the direction of the output light enables 3D measurement of the target's shape. However, 250,000 measurements are required to capture an image of 500 × 500 pixels. Although this is possible using previous mechanical-based light sources, the measurement time is very long.

This article reports use of a high-speed 1250-Hz sweep-frequency light source to measure 3D shape as an 800 × 800 pixel image in 12 minutes, as well as long-range measurement using a low-speed 150-Hz sweep-frequency light source.

2 OFDR Outline

2.1 OFDR Principles

Figure 2 shows the basic principle of OFDR distance measurement. The system is composed of a swept light source, interferometer, collimator lens, and optical receiver.

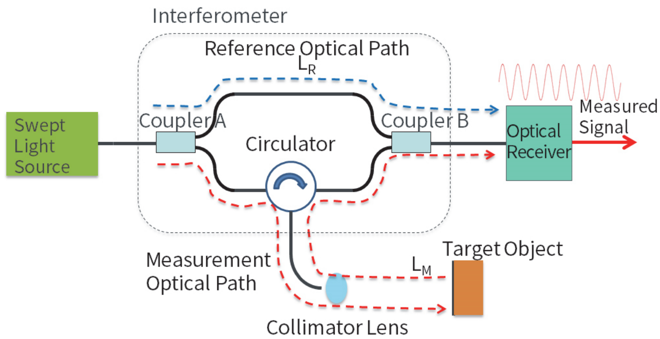

Figure 2 Principles of Distance Measurement Using OFDR

Light output from the swept light source is split into two paths by coupler A. One beam passes as is to coupler B, forming the reference optical path. The other beam passes via a circulator to a collimator lens that outputs the beam into free space to illuminate the target. Reflected light from the target passes back through the collimator lens and circulator (measurement optical path) to coupler B where each optical beam propagated via the reference and measurement paths is combined and passes to an optical receiver for optical-digital conversion.

Although the above description uses the term 'wavelength', since most people use the term 'optical frequency' for simplicity and logical consistency in interferometry terms, this article uses optical frequency instead of wavelength from here on.

The optical frequency of the light output from the swept light source changes linearly over time as expressed by Eq (1)

$$\nu(t) = \nu_0 + k \cdot t \quad (1)$$

where: t is time, $\nu(t)$ is optical frequency, ν_0 is optical frequency at time 0, and k is the sweep speed (Hz/s). Assuming the difference between the reference optical path length L_R and the measurement optical path length L_M including the index is $\Delta L = |L_M - L_R|$, the propagation time delay τ of both paths from the swept light source to the optical receiver is

$$\tau = \frac{\Delta L}{c} \quad (2)$$

where, c is the velocity of light in vacuum.

If E_R and E_M are the field strengths of the optical signals passing through the reference and measurement optical paths, respectively, the interference intensity P detected by the optical receiver is expressed by

$$\begin{aligned} \mathrm{P} &= \left|\vec{E_R} + \vec{E_M}\right|^2 \\ &= \left|E_R e^{i2\pi\nu(t)\cdot t} + E_M e^{i2\pi\nu(t-\tau)\cdot t}\right|^2 \quad (3). \\ &= |E_R|^2 + |E_M|^2 + 2|E_R||E_M| cos\left(2\pi \frac{k\Delta L}{c} t\right) \end{aligned}$$

Assuming the interference signal DC components are filtered out, only the last third term of Eq (3) is observed. In other words, assuming the optical frequency in Eq (1) is swept linearly, the frequency of the electrical signal output from the optical receiver is

$$f_I = \frac{k\Delta L}{c} \quad (4).$$

Accordingly, applying a Fast Fourier Transform (FFT) after sampling the electrical signal will detect a sharp peak at position f_I on the FFT spectrum from which the difference in the lengths of the optical paths ΔL can be calculated using Eq (4).

Moreover, multiple reflection points can be detected as the same number of peaks as points on the FFT spectrum. When there is reflection at the collimator lens face, measuring the spaces between peaks corresponding to the target reflections indicates the distance from the collimator lens to the target object.

From Eq (4), if the sweep speed varies by 1% while sweeping the optical frequency, the FFT peak will have a width of 1%; Since measurement precision drops greatly as the peak becomes wider, maintaining a fixed sweep speed is essential for high-precision measurement. However, the actual light source sweep speed fluctuates greatly during sweeping. Using the Anritsu Devices sweep light source shown in Figure 1, the wavelength changes over time as a sine wave (Figure 3) and the sweep speed varies as a cosine wave due to the time derivative of the wavelength change. Consequently, there is a 13% change in the sweep speed even at the sweep 50% point which appears to be relatively linear (blue segment in Figure 2, $\lambda c - W/4 < \lambda < \lambda c + W/4$).

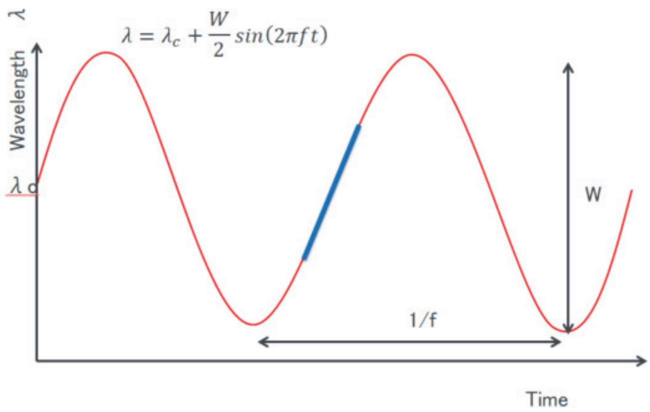

Figure 3 Wavelength Changes at Sweeping

Although it is difficult to control the swept light source sweep speed so that the optical frequency changes linearly, it is possible to use a sampling method and software processing so that the measured optical frequency changes linearly; in other words, the same result can be obtained as the result when the optical frequency interval is fixed. This process is called linearizing.

There are two linearizing methods: Software Linearization, and Hardware Linearization.

2.2 Optical System for Linearization

Figure 4 shows an OFDR optical system including linearization.

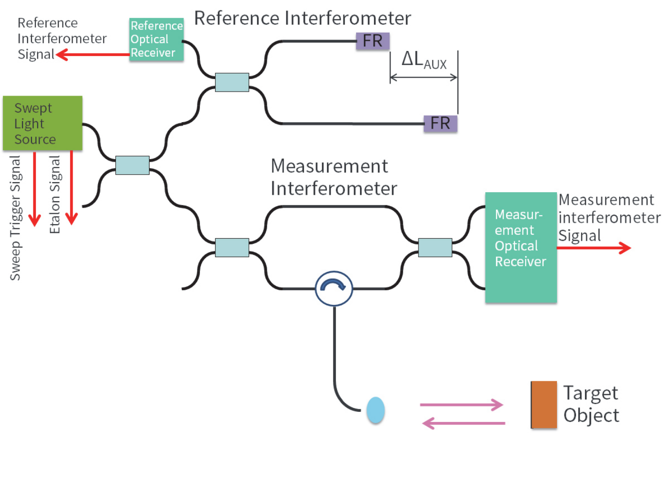

Figure 4 OFDR System with Linearization

In this system, the light output from the swept light source is split into 2 paths by a coupler; however another interferometer for compensation is inserted like the interferometer in Figure 2. In this example, the reference interferometer is a Michelson type using a coupler and Faraday mirrors (FR) as reflecting mirrors. Since the light from each reflecting mirror is inserted to the reference optical receiver in the same polarization state whatever the delay, the system has the merit of filtering-out changes in the interference signal caused by polarization changes.

The reference interferometer signal frequency is found from,

$$f_{AUX} = \frac{2k\Delta L_{AUX}}{c} \tag{5}$$

where, ΔL_{AUX} is the difference in the length of the optical paths including the index. At comparison with Eq (4), the 2 multiplier in the numerator accounts for the ΔL_{AUX} round trip path. Additionally, since the Free Spectral Range (FSR) of the reference interferometer, or–in other words–the interference signal changes for one sine wave, since the required optical frequency is expressed as

$$FSR = \frac{c}{2\Delta L_{AUX}} \tag{6}.$$

Equation (5) can be expressed as

$$f_{AUX} = \frac{k}{FSR} \tag{7}$$

and the right side is an expression where the sweep speed k is equivalent to a multiple of the FSR, or put another way, f_{AUX} can be said to be the frequency of the interfering signal that has a maximum value each time the optical frequency is swept by the FSR.

2.3 Hardware Linearization

If the measurement signal is sampled each time the reference interferometer signal becomes local maximum, the measurement interferometer signal is the data measured each time the optical frequency is FSR swept, and is simply sampled at each fixed optical frequency interval.

This can be implemented by inputting the reference interferometer signal to the sampling clock for the A/D converter. This method is called Hardware Linearization and is used in Optical Coherent Tomography (OCT) because the system is simple and the speed can be increased easily (Figure 5).

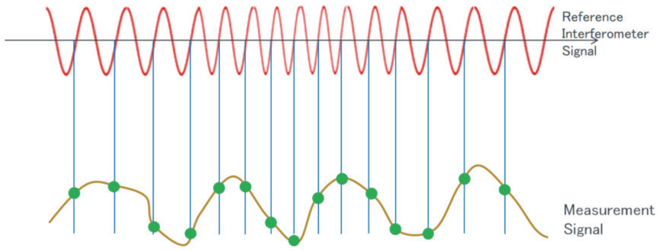

Figure 5 Linearization Principle

When sweeping from optical frequency ν_1 (wavelength λ_1) to optical frequency ν_2 (wavelength λ_2), the number of waves N output from the reference optical receiver is expressed by

$$N = \frac{(\nu_1 - \nu_2)}{FSR} = \left(\frac{1}{\lambda_1} - \frac{1}{\lambda_2}\right)\frac{C}{FSR} \tag{8}.$$

By sampling the reference interferometer signal and the etalon signal as the optical frequency reference at the same time, the optical frequency during the sweep can be accurately measured. Consequently, accurate measurement of ν_1 and ν_2 enables accurate calculation of ΔL_{AUX} from Eq (8) and Eq (6) as

$$\Delta L_{AUX} = \frac{cN}{2(\nu_1 - \nu_2)} = \frac{N\lambda_1\lambda_2}{2(\lambda_2 - \lambda_1)} \tag{9}.$$

Additionally, the maximum frequency when FFT-processing sampled data is equivalent to ΔL_{AUX} and the positions of reflection points can be found from the positions of frequencies where peaks are detected by proportion calculations. The measurement resolution Δz for reflection point positions is found from Eq (9) as

$$\Delta z = \frac{c}{2(\nu_1 - \nu_2)} = \frac{1}{2}\frac{\lambda_1\lambda_2}{\lambda_2 - \lambda_1} \cong \frac{1}{2}\frac{\lambda_c{}^2}{\Delta\lambda} \tag{10}$$

where, λc is the sweep center wavelength, and $\Delta\lambda$ is the wavelength sweep width.

2.4 Software Linearization

This section explains Software Linearization. In this method, the reference interferometer signal and the measurement interferometer signal are sampled by the A/D converter at the same time interval. And, the measurement interferometer signal is linearized with the frequency of the reference interferometer signal as a scale so that the measurement interferometer signal is to be linear with respect to the optical frequency. The actual method is described below.

First, Hilbert transformation is applied to the reference interferometer signal to calculate the phase data which, since it changes repeatedly between $-\pi$ and $+\pi$, is used to calculate the consecutive phase P_R by adding 2π to the phase each time it jumps from +π to −π (Figure 6). The continuous phase is an amount that increases by 2π each time the optical frequency is swept by the FSR of the reference interferometer and is proportional to the optical frequency.

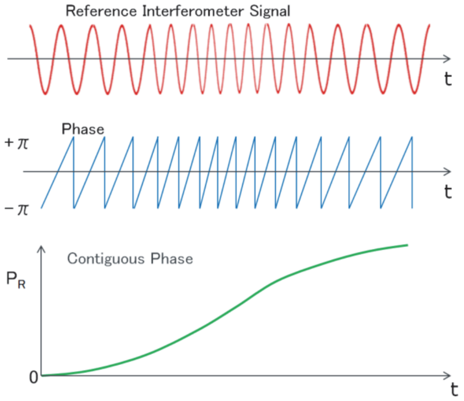

Figure 6 Calculated Phase of Reference Interferometer Signal

Next, the continuous phases are divided equally and the intensity of the measurement interferometer signal at each divided point is extracted (green circles in Figure 7). Although the extracted data is not equidistant on the time axis, the sampled data is equidistant on the optical frequency axis. Applying FFT to the extracted data enables monitoring of the sharp peaks at the frequency positions for reflection points.

Hardware and software linearization each have good and bad points. Generally, software linearization is used when high accuracy is required, and hardware linearization is used for applications where high speed is important.

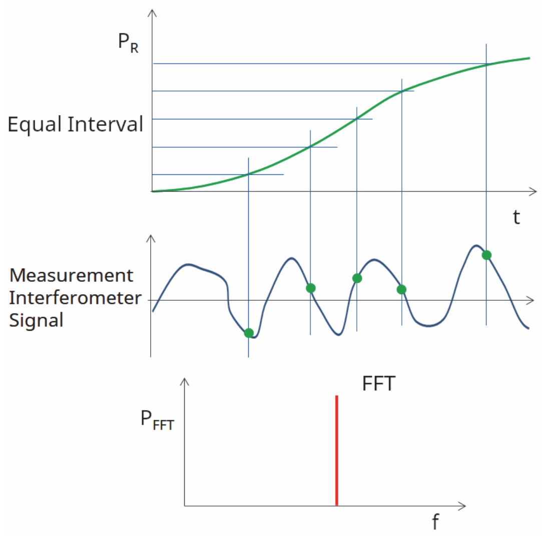

Figure 7 Data Extraction

Figure 8 shows the etalon and measurement interferometer signals sampled at equal time interval. Figure 9 shows the signals sampled by hardware linearization. At measurement at equal time intervals, the etalon peak spaces are wider further from the sweep center due to become the low sweep speed as shown Figure 8. However, with hardware linearization, the measured etalon signal has the same peak spaces due to sampling at the same optical frequency intervals.

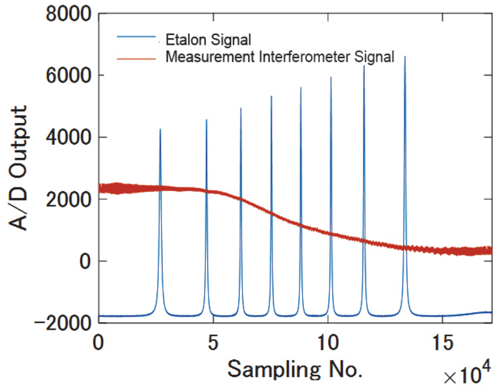

Figure 8 Signals Sampled at Same Time Interval

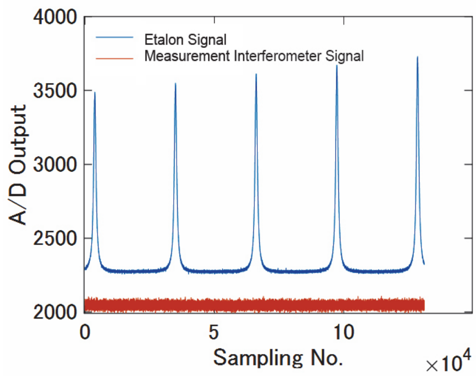

Figure 9 Signals Sampled Using Hardware Linearization

Figure 10 shows the FFT processing result for the measurement interferometer signal sampled by hardware linearization. The reflection peaks from the Angled Physical Contact (APC) face of the fiber connected to the collimator lens, the collimator lens face, and the target object can all be observed.

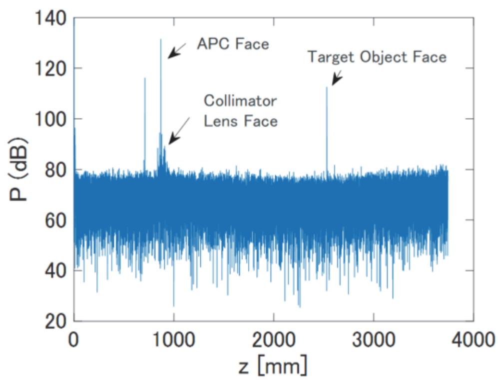

Figure 10 FFT Spectrum

3 3D Shape Measurement

3.1 External View of Demonstration Unit

Figure 11 shows the external appearance of the prototype 3D shape measuring instrument. It uses hardware linearization to support longer-distance measurement. Light from the collimator lens is output to scan the target and reflected light returning from the target is focused by the collimator lens to measure the distance from the target. If successive measurement are made while the light output from the collimator lens scans up/down and left/right, the shape of the target can be measured. Consequently, the collimator lens is mounted on an automatic 2-axis revolving stage (Figure 11 right inset).

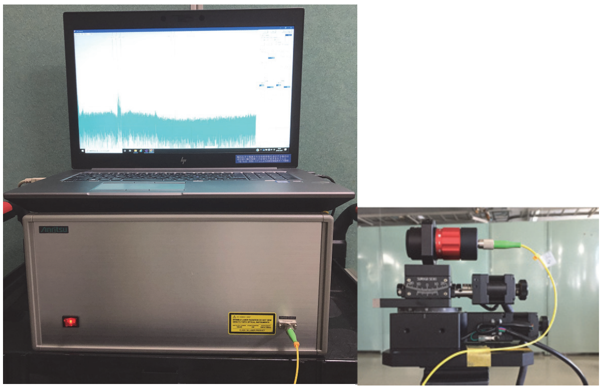

Figure 11 3D Shape Measuring Instrument

The distance origin (frequency 0) calculated from the FFT result is located where the reference optical path length and measurement optical path length are at the same position, but sometimes this location may change due to the impact of external environmental conditions, such as the fiber temperature. Consequently, to improve the accuracy further, the reflection peak from the APC facet connected to the collimator lens is monitored and the distance from the target is measured using that location as the origin.

The swept light source has a sweep center wavelength of 1550 nm and a sweep frequency of 1250 Hz.; the wavelength sweep width is 40 nm and a range of 20 nm near the center within this is sampled.

To evaluate the distance measurement precision, a black-faced alumite-processed aluminum block is positioned about 50 cm from the collimator lens and the change in the distance between the collimator lens and the block is monitored. Figure 12 shows the measurement results with a histogram. The distance resolution calculated from Eq (10) is 60 μm but the position detection precision for reflection peaks on the FFT spectrum (Figure 10) greatly exceeds the resolution. The standard deviation in the measured distance for 10 s (about 13,000 measurements) is 0.2 μm. In other words, the distance measurement precision of the 3-D shape measuring instrument is 0.2 μm. Commercial positioning sensors for distance measurements of 50 cm or more have a measurement precision of about 5 μm, which this 3-D shape measuring instrument greatly exceeds.

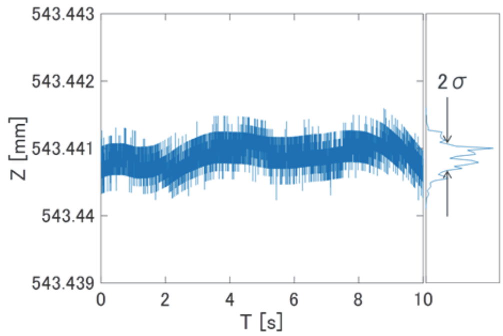

Figure 12 Distance Measurement Result Time Variation and Histogram

3.2 Shape Measurement Results

Figure 13 shows the measurement results for a model airplane positioned at a distance of about 2 m. The measurement ranges in the vertical and horizontal directions are 18° respectively, and the number of pixels is 800 × 800 pixels. The scanning progresses horizontally step-by-step at every 800 vertical measurements and requires just 12 minutes to complete a 3D high-resolution measurement of 800 × 800 pixels. The measurement time includes the time taken for the vertical auto-stage to return to the origin and could theoretically be shortened to 512 s ([800 × 800]/1250 Hz).

For clarity, this model is shown isometrically; the model shape including floor irregularities can clearly be measured with high precision.

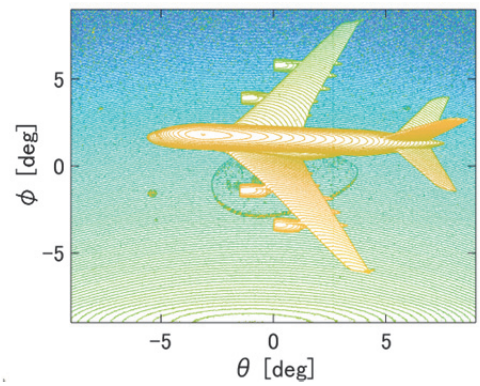

Figure 13 Measurement Results for Model Aircraft

Figure 14 shows the result from measuring the surface of a ¥100 coin. The image is 400 × 400 pixels and the cross-section is shown in Figure 15. The coin surface is clearly deeper near the central region. The heights of the 1, 0, and 0 relief characters are about 100 μm.

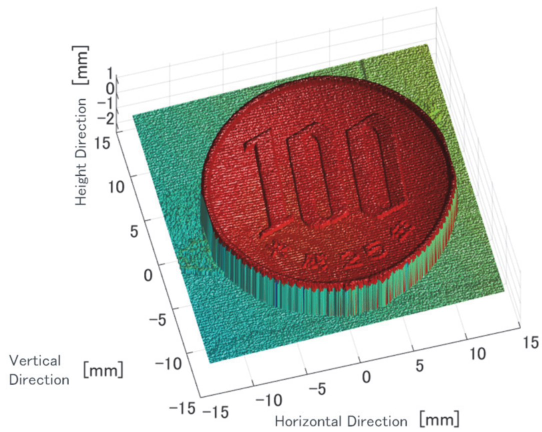

Figure 14 Measurement Results for ¥100 Coin

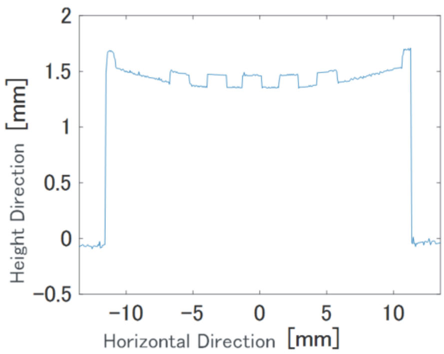

Figure 15 Cross-Section of ¥100 Coin

Sometimes conservation and repair of cultural artefacts, such as paintings and sculptures, requires the creation of replicas that accurately reproduce the damage and irregularities in the objects. As a demonstration, we measured the surface 3D shape of an acrylic painting (Figure 16).

Figure 16 Measured Acrylic Painting

Figure 17 shows the painting measurement results as an image of 800 × 800 pixels. The furthest part from the collimator lens is indicated in blue while the nearest parts are in red. Although the painting appears to be flat, there is clearly a concave area near the center.

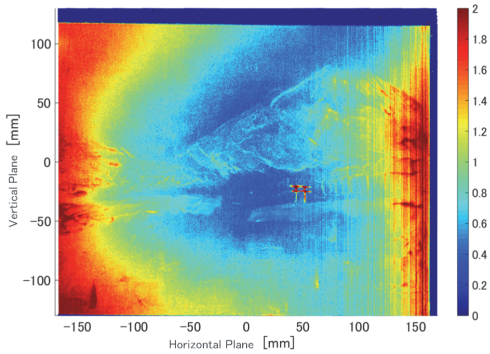

Figure 17 Acrylic Painting Surface Measurement Results

Figure 18 shows a magnified view of the Shinto torii gate near the painting center. The 3-cm rectangular torii has a clear height of about 1 mm. Printing this measurement result using a 3D printer would create an accurate replica.

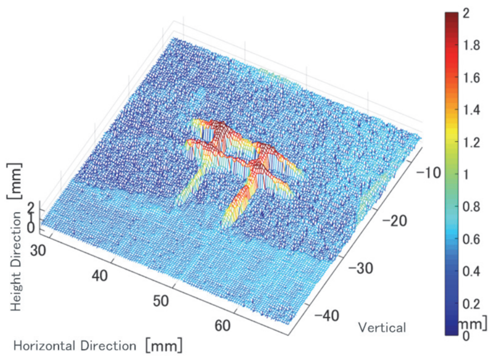

Figure 18 Enlargement of Torii Gateway

Next, we measured a corner of our laboratory (Figure 19). The distance was about 2 m. The scan was 18° in the vertical plane and 24° in the horizontal place to produce an image of 800 × 800 pixels as shown Figure 20. The difference between the nearest and furthest point was about 1 m and the depth of field was 1 m for a distance of 2 m.

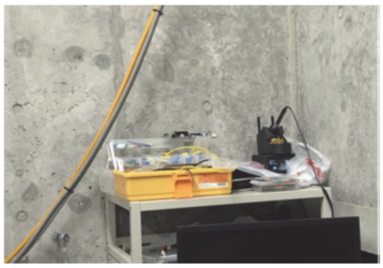

Figure 19 Laboratory Corner

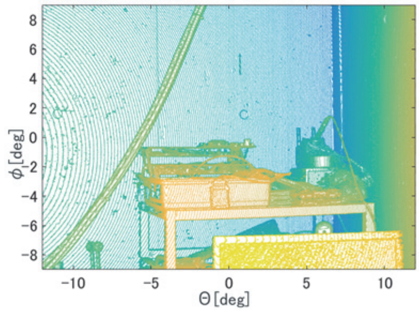

Figure 20 Laboratory Corner Measurement Results

4 Long-Distance Measurement

Finally, to test long-distance measurement, we measured the distance between two adjacent buildings separated by about 20 m in the N-S direction (Figure 21). Light was projected from an office in the northern building onto window glass on the side of the southern building and the reflected light re-entering the window of the northern building was monitored. The swept light source had a sweep frequency of 150 Hz with a long coherence length.

The blue band in Figure 22 shows the change in the distance measured over a 45-minute period. When the distance from the reflection point is large, the collimator lens collects less light so the Signal to Noise (S/N) ratio of the reflection peak becomes smaller and the measurement precision drops. However, this measurement trial confirmed that the standard error was 23 µm over a 20-m distance. To clarify the change in the distance, we plotted the mean distance for 100 measurements as the red line in Figure 22, showing the building distance increased by 200 µm during the 45-minute measurement period. Since the measurements were made during the evening when air temperature was dropping, we believe the temperature gradient between the north and south sides of the buildings might cause the buildings to tilt slightly north and south to increase the distance very slightly.

Figure 21 On-site Measurement Between Buildings

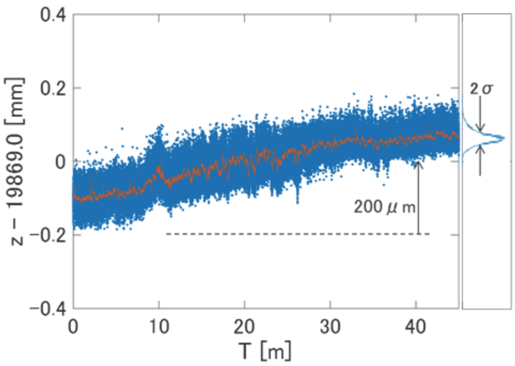

Figure 22 Results of Measurement Between Buildings

If distances from fixed points to buildings, bridges, cliffs, etc., can be measured with high precision, we may be able to obtain more precise data on ground subsidence and building inclination. In addition, measurements at 150 Hz can also measure building frequency characteristics to help detect the degree of structural aging. We believe that long-distance measurements using OFDR could help with disaster-prevention measures.

5 Conclusions

We have developed an OFDR distance measurement system for high-precision measurement of commonly used distances ranging from several cm to meters. We used a high-coherence wavelength swept light source developed by Anritsu Devices as the key light source for OFDR. By making use of this coherence length we were able to measure absolute distance ranges from 0 mm to several meters with an accuracy of 0.2 µm at a measurement frequency of 1250 Hz. In addition, we confirmed measurements up to a distance of 20 m with 23-µm accuracy using a low-speed version of the wavelength swept light source at a frequency of 150 Hz. These OFDR-type distance measurement systems can be used to configure 3D shape measurement systems by adding a mechanism for scanning in the measurement direction to produce high-accuracy 800 × 800-pixel images of 3D shapes in 12 minutes.

References

1) T. Tanimoto, S. Mattori, H. Kameyama, F. Otagaki, and H. Otateme, "Wavelength tunable laser," Japanese Patent No. 3069643 (in Japanese)
2) K. Nakamura, S. Morimoto, and T. Nakayama, "Single-Mode and Mode-Hop-Free Wavelength Sweep Light Source with Range of Over 160 nm and High Swept Frequency," IEEE Photonics Technology Letters, Vol. 22, No. 19, Oct. 2010.
3) K. Nakamura, M. Koshihara, T. Saitoh, K. Kawakita: "High-Coherence Wavelength Swept Light Source", Anritsu Technical Review No.25 September 2017
4) Optical Coherence Tomography, Technology and Applications, Second Edition, W. Drexler, J. G. Fujimoto, Eds., Springer (2015).

Author

Takanori Saitoh
Applied Light Source
Development Department
Device Development Center